



# Elevated nitrate simplifies microbial community compositions and interactions in sulfide-rich river sediments

Enze Li<sup>a,b,1</sup>, Tongchu Deng<sup>a,b,1</sup>, Lei Yan<sup>a,b</sup>, Jizhong Zhou<sup>c</sup>, Zhili He<sup>d</sup>, Ye Deng<sup>e</sup>, Meiyang Xu<sup>a,b,\*</sup>

<sup>a</sup> Guangdong Provincial Key Laboratory of Microbial Culture Collection and Application, Guangdong Institute of Microbiology, Guangdong Academy of Sciences, Guangzhou 510070, China

<sup>b</sup> State Key Laboratory of Applied Microbiology Southern China, Guangzhou 510070, China

<sup>c</sup> Institute for Environmental Genomics, University of Oklahoma, Norman, OK 73019, USA

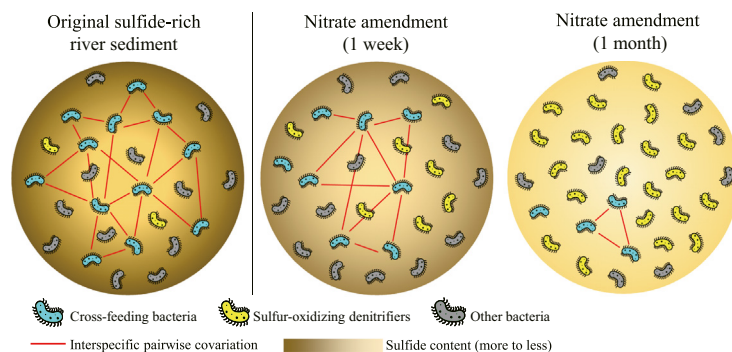
<sup>d</sup> Environmental Microbiomics Research Center, School of Environmental Science and Engineering, Southern Marine Science and Engineering Guangdong Laboratory (Zhuhai), Sun Yat-sen University, Guangzhou 510006, China

<sup>e</sup> Research Center for Eco-Environmental Sciences, Chinese Academy of Sciences, Beijing 100085, China

## HIGHLIGHTS

- Nitrate led to a functional convergence at sulfide oxidation and denitrification.
- Resulting sediments were depleted of sulfide and Fe(II) after 1 month.
- Resulting microbial communities underwent a significant loss of biodiversity
- Microbial interactive networks were mostly sustained by cross-feeders.

## GRAPHICAL ABSTRACT



## ARTICLE INFO

### Article history:

Received 27 April 2020

Received in revised form 3 August 2020

Accepted 3 August 2020

Available online 4 August 2020

Editor: Ewa Korzeniewska

### Keywords:

River sediment

Nitrate pollution

Denitrification

Community simplification

Functional convergence

## ABSTRACT

Excessive nitrate in water systems is prevailing and a global risk of human health. Polluted river sediments are dominated by anaerobes and often the hotspot of denitrification. So far, little is known about the ecological effects of nitrate pollution on microbial dynamics, especially those in sulfide-rich sediments. Here we simulated a nitrate surge and monitored the microbial responses, as well as the changes of important environmental parameters in a sulfide-rich river sediment for a month. Our analysis of sediment microbial communities showed that elevated nitrate led to (i) a functional convergence at denitrification and sulfide oxidation, (ii) a taxonomic convergence at *Proteobacteria*, and (iii) a significant loss of biodiversity, community stability and other functions. Two chemolithotrophic denitrifiers *Thiobacillus* and *Luteimonas* were enriched after nitrate amendment, although the original communities were dominated by methanogens and syntrophic bacteria. Also, serial dilutions of sediment microbial communities found that *Thiobacillus thiophilus* dominated 18/30 communities because of its capability of simultaneous nitrate reduction and sulfide oxidation. Additionally, our network analysis indicated that keystone taxa seemed more likely to be native auxotrophs (e.g., syntrophic bacteria, methanogens) rather than dominant denitrifiers, possibly because of the extensive interspecific cross-feeding they established, while environment perturbations probably disrupted that cross-feeding and simplified microbial interactions. This study advances our understanding of microbial community responses to nitrate pollution and possible mechanism in the sulfide-rich river sediment.

© 2020 Elsevier B.V. All rights reserved.

\* Corresponding author: 100, Central Xianlie Road, Guangzhou 510070, China.

E-mail addresses: [eli6@hawk.iit.edu](mailto:eli6@hawk.iit.edu) (E. Li), [tongchudeng2013@126.com](mailto:tongchudeng2013@126.com) (T. Deng), [jzhou@ou.edu](mailto:jzhou@ou.edu) (J. Zhou), [hezili@mail.sysu.edu.cn](mailto:hezili@mail.sysu.edu.cn) (Z. He), [yedeng@rcees.ac.cn](mailto:yedeng@rcees.ac.cn) (Y. Deng), [xumy@gdim.cn](mailto:xumy@gdim.cn) (M. Xu).

<sup>1</sup> Equal contributions.

## 1. Introduction

Nitrate is one of the essential nitrogen components in the biosphere. To meet the increasing demands of food and energy, increasing quantities of nitrate have been produced every year (Xia et al., 2018). Rivers are the central surface water ecosystems and serve as water supply, irrigation and transportation systems. The riverine nitrate source can be various including anthropogenic inputs and natural processes (Shang et al., 2020). Excess input of nitrate from agriculture, wastewater facilities and other systems triggers widespread nitrogen pollution, which has become an increasing issue due to its impacts on human health and aquatic ecosystems (Cheng and Basu, 2017; Kazakis et al., 2020; Wu and Sun, 2016).

The distributions, community structures and activities of microorganisms affect the transportation and transformation of nitrate in rivers. River sediments are dominated by anaerobes and are characterized rich in reductive substances (Falkowski et al., 2008). Since oxygen is difficult to permeate into deep sediments, nitrate ranks the best electron sink in association with anaerobic oxidation of organic matters, sulfide and ferrous iron (Burgin and Hamilton, 2007). That explains why nitrate can influence so many microorganisms and why sediments are often the hotspot of biological denitrification (Cheng and Basu, 2017).

A number of studies have demonstrated that denitrification rates in river sediments were positively correlated with nitrate concentration, and elevated nitrate caused certain positive effects in sulfide-rich river sediments, such as odor control, simultaneous oxidation of sulfide and ferrous ion, and a suppression of euxinia (He et al., 2018, 2017). Our previous study also identified an enrichment of functional genes involved in nitrogen (e.g. *nir*, *nif*, *nor* and *nas*) and sulfur cycles (e.g. *sox*, *dsr*, *apr* and *sir*) when sulfide-rich sediment microorganisms were exposed to elevated nitrate (Xu et al., 2014). These studies however, focused either on physiochemical improvements or nitrate dose control, rather than considering nitrate as a prevailing contaminant and looking into native microorganisms from an ecological view.

Biodiversity increases community resistance to environmental perturbations (Evans et al., 2017; Griffiths and Philippot, 2013; Isbell et al., 2015; Xun et al., 2019), and nitrate pollution or amendment is always associated with biodiversity loss (He et al., 2018). It was found that microorganisms in nature co-exist as communities, and species interactions are essential to stabilize their composition and functionality (Donaldson et al., 2016). However, little is known about the microbial adaptations to elevated nitrate in terms of community structure, function and covariation networks.

In this study, we aimed to understand the response of microbial communities to nitrate pollution in the river sediment. It was hypothesized (i) that significant biodiversity loss would be observed because of the enrichment of denitrifiers; (ii) that the overall community functions would converge at nitrate reduction coupled with sulfide oxidation; and (iii) that the microbial covariation networks would be remodeled based on metabolic behaviors of denitrifiers. To test those hypotheses, nitrate amendment was employed to lab-scale river sediments rich in organic matter and sulfide, and microbial community succession and environmental conditions were monitored for 32 days. This study provides new insights into possible microbial mechanisms of nitrate-induced biogeochemical cycling in the river sediment.

## 2. Results

### 2.1. Nitrate amendment induced AVS and Fe(II) oxidation

Five sampling timepoints divided the incubation into four stages. Each stage of the nitrate group had distinct physiochemical features. On Day 4, nitrate was consumed by 13.8% (from 7.74 to 6.82 mM,  $P < 0.001$ ) but little nitrite ( $< 0.01$  mM) was produced (Fig. S1A). Similarly, acid volatile sulfide (AVS) was consumed by 19.3% (from 0.47 to 0.38 mM,  $P < 0.001$ ) and little sulfate (from 0.029 to 0.033 mM) accumulated, suggesting an incomplete AVS oxidation (Fig. S1B). Nitrate and sulfate levels of control sediment were too low to be detected ( $< 1$   $\mu$ M) while AVS was around 0.53 mM. On Day 8, nitrate and nitrite levels barely changed but sulfate concentrations doubled from 0.04 to 0.09 mM ( $P < 0.001$ ), which substantiated AVS oxidation. Nitrate-amended sediments on Day 16 featured a further nitrate reduction and coupled AVS oxidation, with a slight nitrate consumption (by 8.1%,  $P < 0.001$ ), a significant AVS consumption (by 56.96%,  $P < 0.001$ ) and a drastic sulfate accumulation (by 221%,  $P < 0.001$ ).

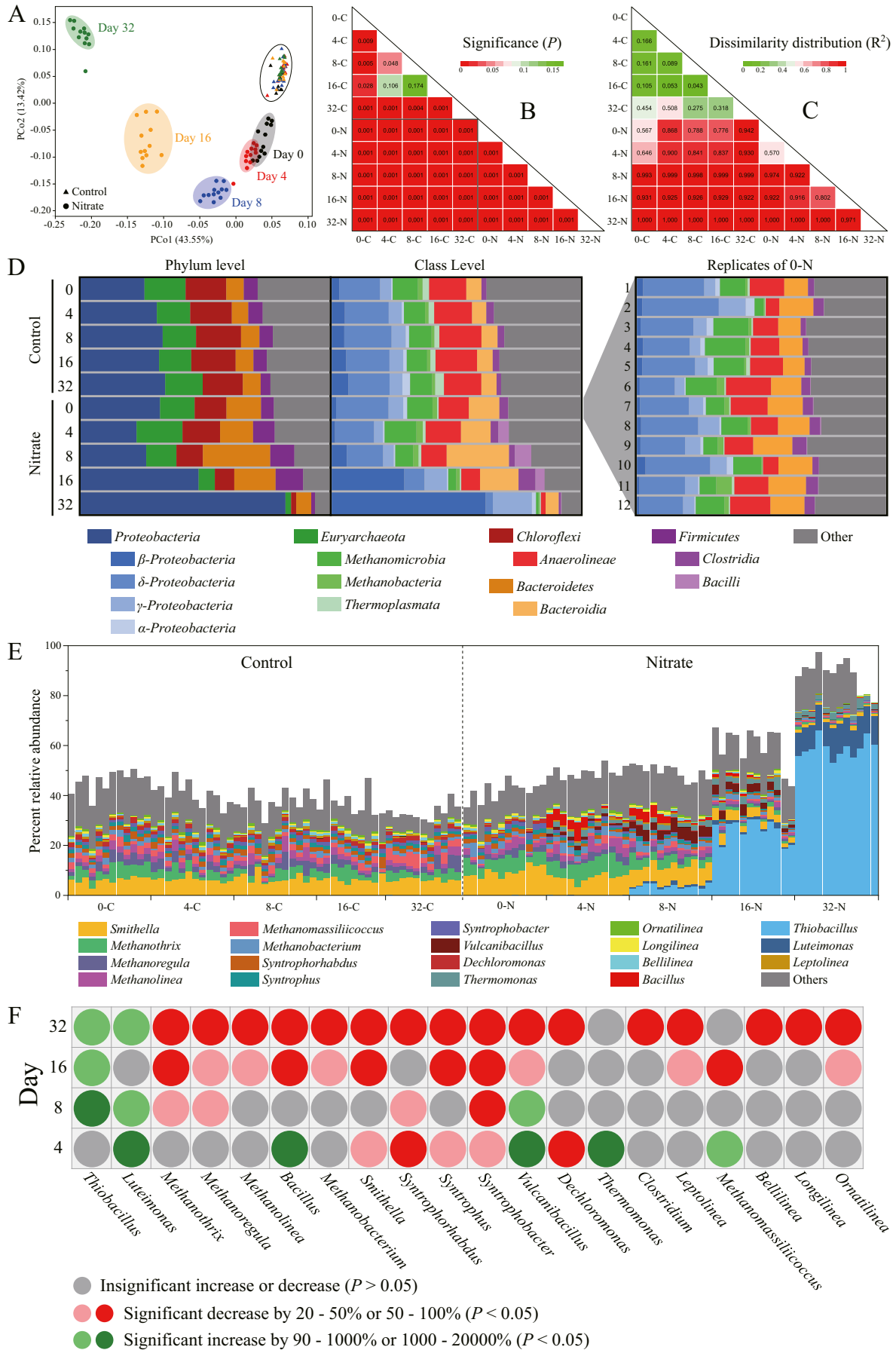
This trend continued to the final stage (Day 16–32), except that Fe (II) participated in nitrate reduction. By the end of the incubation, AVS was too depleted ( $-0.022$  mM) to sustain nitrate reduction and instead a drastic consumption of ferrous ion took place (from 3.403 to 0.417 mM, by 87.75%). Interestingly, the levels of total acid-soluble iron, i.e. the sum of Fe(II) and Fe(III), changed slightly ( $-4.30\%$ ) so that most Fe(II) was oxidized to Fe(III) (Fig. S1D). Fe(II) consumption supported AVS depletion since Fe(III) spontaneously oxidizes AVS and thus Fe(III) accumulation indicated little AVS remaining. In summary, 0.450 mM AVS and 2.99 mM Fe(II) were oxidized throughout the incubation, yielding 0.404 mM sulfate and 2.559 mM Fe(III) respectively. Correspondingly, 2.51 mM nitrate was reduced, yielding merely 0.094 mM nitrite. It is noted that more nitrate in stoichiometry was consumed than the sum of sulfate and Fe(III) production if nitrate was denitrified to nitrogen gas.

### 2.2. Nitrate amendment simplified community composition

PCoA well substantiated the community dissimilarities between two groups (Fig. 1A), where the nitrate group fell into distinct subgroups per sampling time and the control group showed no significant difference over time. For the nitrate group, a longer incubation led to a larger dissimilarity between subgroups, suggesting that the notable community succession was in response to elevated nitrate but not to the one-month incubation. We performed one-way ANOSIM to further compare the pairwise dissimilarities between subgroups with respect to dissimilarity significance ( $P$ ) and distribution ( $R^2$ ). For convenience, we used “C” to represent the control sediment, and “N” to represent the nitrate-amended sediment. For example, “4-C” referred to the control sediment on Day 4. Most subgroups were statistically different from each other except 4-C vs. 16-C and 8-C vs. 16-C (Fig. 1B). Any pairwise dissimilarity between C–N and N–N subgroups was significant ( $P < 0.001$ ), as ANOSIM suggested. In contrast, most control subgroups had comparable within- and between-subgroup dissimilarities (Fig. 1C).

The relative abundance of categorized OTUs at the phylum or class level suggested a progressive dominance of *beta-Proteobacteria* in nitrate-amended sediments, while classes *Delta-Proteobacteria*, *Anaerolineae* and Phylum *Euryarchaeota* dominated the control,

**Fig. 1.** Metrics concerning community successions. In the PCoA plot based on Bray-Curtis distance (A), control communities were rather time-steady but nitrate communities were progressively drifting from previous states. Samples falling out of the circle were too divergent from other replicates and were excluded from further analysis. Communities of all subgroups except the pairs of 4-C/16-C and 8-C/16-C were significantly different ( $P < 0.05$ ) in the significance matrix of one-way ANOSIM (B), especially those in the N–N and C–N areas ( $P < 0.001$ ). Most control communities had comparable dissimilarities within and among subgroups, while dissimilarities among nitrate subgroups were much greater than dissimilarities within nitrate subgroup (C). The categorized taxonomic composition at the phylum and class levels suggested a stepwise enrichment of *beta-proteobacteria* occurring to nitrate sediment communities (D). In particular, genera *Thiobacillus* and *Luteimonas* outcompeted other genera (E, unclassified genera were left blank) and became dominant (F).



accounting for 17.50%, 15.43% and 11.37%, respectively (Fig. 1D). The enrichment of *Beta-proteobacteria* (from 1.79% to 61.81%, ~35 folds) accounted for the dissimilarities among nitrate subgroups. Only ~1/3 of total 4990 OTUs could be assigned to a specific genus (Fig. 1E). Among those, syntrophic bacteria (e.g. *Smithella*, *Syntrophorhabdus*, *Syntrophphus* and *Syntrophobater*) and methanogenic archaea (e.g. *Methanothrix*, *Methanoregula*, *Methanolinea*, *Methanobacterium* and *Methanomassiliicoccus*) dominated control and early nitrate communities. Compositions of control communities were rather time-steady so we only screened genera significantly changing over time within the nitrate group by paired *t*-test. We found that most genera were gradually outcompeted alongside the rise of genus *Thiobacillus* and *Luteimonas* (Fig. 1F), and the core microbiomes of late nitrate subgroups (i.e., 16-N and 32-N) greatly differed in taxonomy and abundance from control and the early nitrate subgroups.

### 2.3. Nitrate amendment simplified covariation network

Ten networks based on Spearman's correlation coefficient were constructed to identify possible interactions in a microbial community. Key network topologies were listed in Table S1, from which we selected network size, modularity and connectivity to correlate three community metrics (Fig. 2). Sizes of control networks remained time-steady ( $428.8 \pm 23.7$  nodes,  $P \gg 0.05$ ) while nitrate networks kept shrinking, from 308 (Day 0) to 94 nodes (Day 32), meaning that fewer OTU pairs were generating significant abundance covariations. Such changing patterns applied to all metrics in Fig. 2 that elevated nitrate was simplifying

community compositions (with respect to richness and  $\alpha$ -diversity) and microbial interactions. To visualize this simplification, all networks were plotted (Fig. 3). The Fruchterman Reingold layout well exhibited the shrinking sizes of nitrate networks, while the Yifan Hu layout emphasized the decreasing modularity and node-node interactions.

Putative keystone nodes referred to those of great network connectivity, either within a module (i.e. module hub) or among modules (i.e. connector). Their taxa were therefore putative keystone taxa. We plotted the distribution of keystone nodes in Fig. S2A. Of all the 3352 nodes, most were insignificant peripherals (97.67%), 44 were module hubs and 34 were connectors (Table S2). No network hub was detected. When correlating node significance to OTU relative abundances (Fig. S2B), we found that abundance did not necessarily determine its network connectivity, although keystone nodes turned to be sparse OTUs. Of the 78 keystone nodes, 31 were rare (<0.1% relative abundance), 27 were moderately rare (0.1–0.5%), 13 were moderately abundant (0.5–1%), and only 7 were abundant (>1%). In addition, the relative abundances of module hubs and connectors indicated no significant difference ( $P > 0.05$ ).

To investigate the putative keystone taxa, we prepared a phylogenetic tree that indicated (i) all the putative keystone taxa at the phylum or genus level; (ii) their phylogenetic distance calculated by the neighbor-joining method; and (iii) their keystone type (Fig. S3). Most keystone nodes (85.5%) could be assigned to a phylum but only 28.9% could be assigned to a genus. Members of phylum *Proteobacteria* (e.g. genus *Smithella* and *Syntrophorhabdus*) and *Chloroflexi* (e.g. genus *Bellilinea*, *Leptolinea* and *Pelolinea*) constituted the majority of keystone taxa. Genus *Smithella* in particular, was found highly interactive in networks

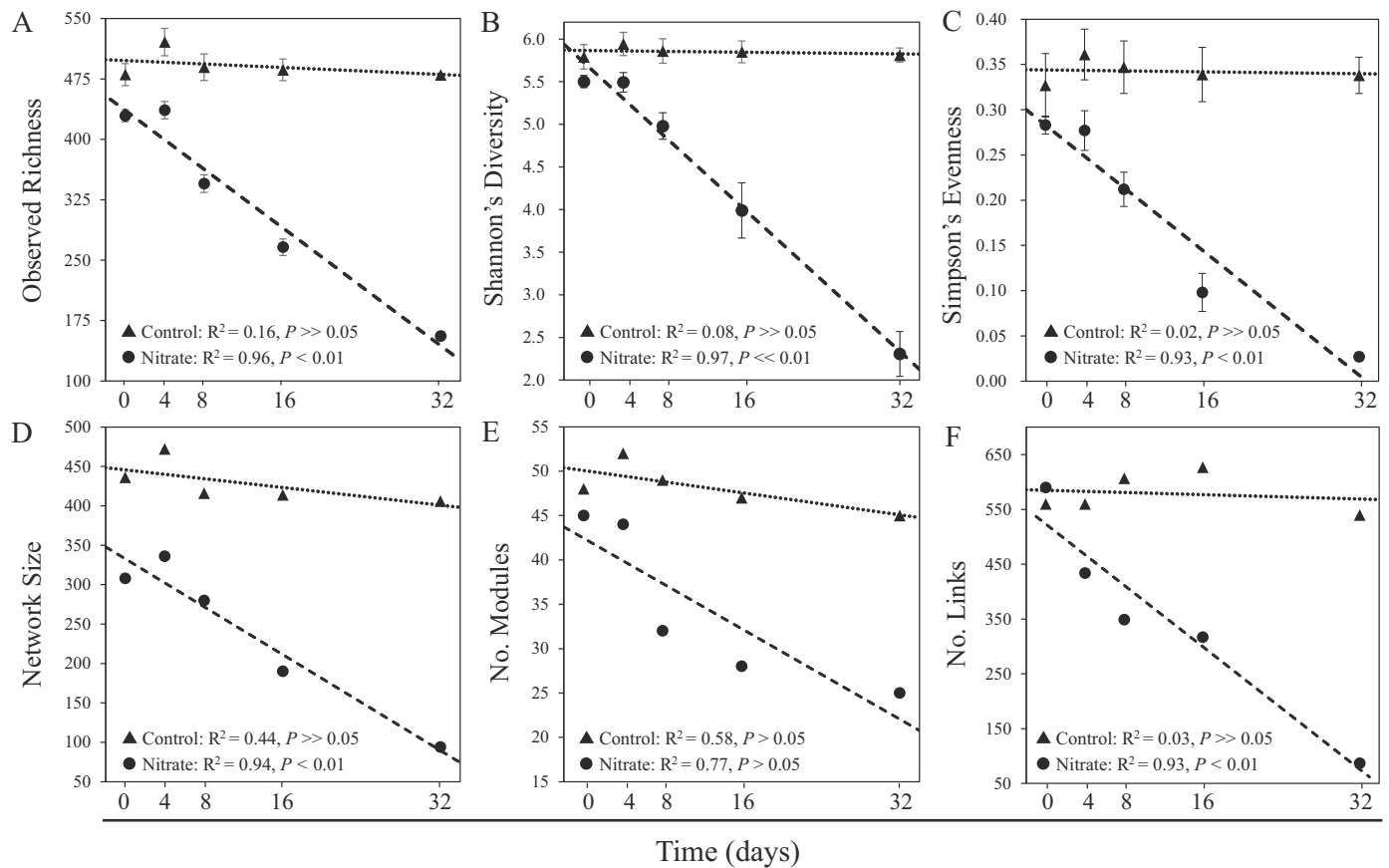


**Fig. 2.** Comparison of community and network metrics. (A) Number of OTUs present in more than 8 out of 12 sediment replicates for each subgroup, (B) Shannon's diversity, (C) Simpson's evenness, (D) number of nodes of each constructed network per subgroup, (E) number of modules and (F) number of links. When referring to network modularity and node connectivity, we focused on modules consisting of more than 5 interconnected nodes. (A), (B) and (C) were calculated based on bootstrap method ( $N = 1000$ ).  $R^2$  and  $F$ -significance ( $P$ ) were calculated by regression analyses.

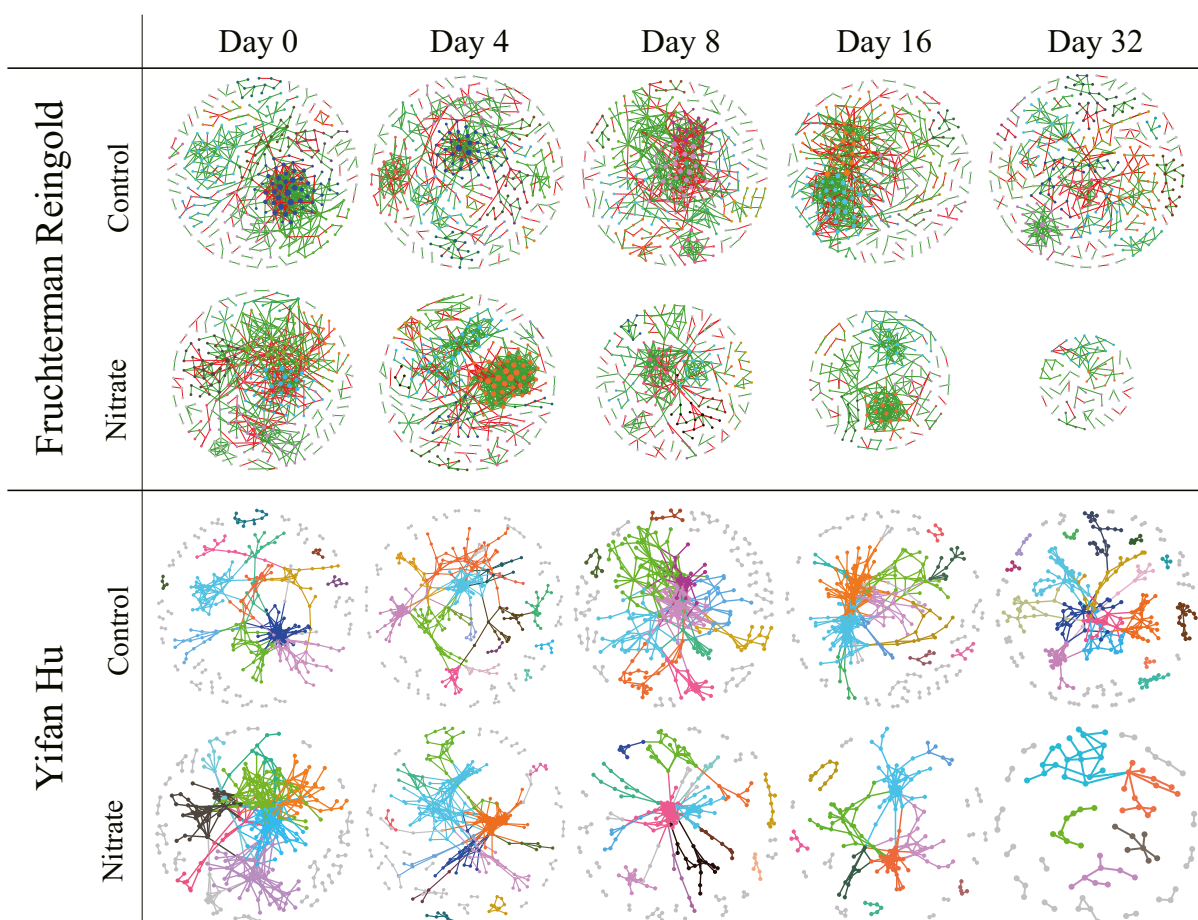


**Fig. 3.** Networks based on 12 replicates were constructed by the RMT-MENA program. Fruchterman Reingold layout exhibited the shrinking nitrate networks. Node size was proportional to its degree. Modules consisting of over 5 nodes were randomly colored, the rest left grey. Positive covariations were colored green and negative covariations were colored red. For convenience, we unified the node density so that network sizes could be directly read from the diameter. Yifan Hu layout emphasized the network connectivity. Nodes and links of the same module shared the same color, and all nodes were in a uniform size. In summary, nitrate networks were getting smaller and simpler. (For interpretation of the references to color in this figure legend, the reader is referred to the web version of this article.)

since 5 OTUs derived from *Smithella* were keystone nodes. In addition, four keystone taxa were methanogenic archaea (Lee et al., 2015), members of genus *Methanolinea*, *Methanotrith*, and *Methanobacterium*.

Generally, the number of keystone nodes decreased as the nitrate amendment proceeded longer (Fig. S4). That is, the network simplification occurred alongside the loss of keystone taxa. Recall that *Thiobacillus* was barely detectable in the control communities (<0.02% relative abundance) but dominated the late nitrate communities (~60.88%). However, it was not a keystone genus, showing no significant covariations in any network (Table S3).

#### 2.4. Predictive functional converge after nitrate amendment

In FAPROTAX, most OTUs (>90.7%) failed to associate with either N- or S-metabolism. This low coverage is not a surprise because FAPROTAX database only collects information of pure cultures with experimentally confirmed functions (Louca et al., 2016). In the absence of favorable electron acceptors, control communities were rich in methanogens (Fig. S5A), which were archaea in the phylum *Euryarchaeota*. The numbers of putative nitrate reducers (e.g., members of genus *Nitrospira*, *Bacillus*, *Paracoccus*) and sulfate reducers (e.g., members of genus *Syntrophobacter*, *Desulfococcus*, *Desulfobulbus*, *Desulfovibrio*) were comparable (Fig. S5B, C). For nitrate communities, the number of putative nitrate reducers kept decreasing, which contradicted the drastic nitrate reduction possibly because the actual nitrate reducers were yet to be collected in the FAPROTAX database. Members of genus *Thiobacillus*,

*Paracoccus*, *Sulfuricurvum* or *Acidithiobacillus* were putative AVS oxidizers and *Thiobacillus* in particular, was assigned to “dark-sulfide-oxidation” and “dark-oxidation-of-sulfur-compounds”.

In PICRUSt, we focused on the changes of gene copy number based on a normalized PICRUSt table (KEGG Orthology Level 2 and 3). Each sample was rarefied to an equal sum of predicted gene copies so that the copy number of each functional item represented its strength. When analyzing the general metabolism (ko09100, Level 2), the late nitrate communities (16-N and 32-N) exhibited the greatest difference from the rest. Five orthologues (ko09102, 09104, 09106-09108) were enriched and four (ko09101, 09109-09111) were suppressed (Fig. 4). Within ko09102 (energy metabolism), nitrogen metabolism had higher background abundances (~25,000 copies per community) than sulfur metabolism (~10,500) and were more enriched after nitrate amendment (Fig. S5E, F).

#### 2.5. *Thiobacillus thiophilus* became the best competitor in enriched communities

The community of control sediments was serially diluted and cultured anaerobically in the NS media where nitrate was the sole electron acceptor and sulfide was the sole electron donor. This is to enrich bacteria having a complete or partial metabolic chain from sulfide, the initial e-donor to nitrate, the terminal e-acceptor. The dominance of *Thiobacillus* reappeared in 20 out of 38 communities (Fig. 5A) though it was initially sparse (<1.3% relative abundance). This enrichment

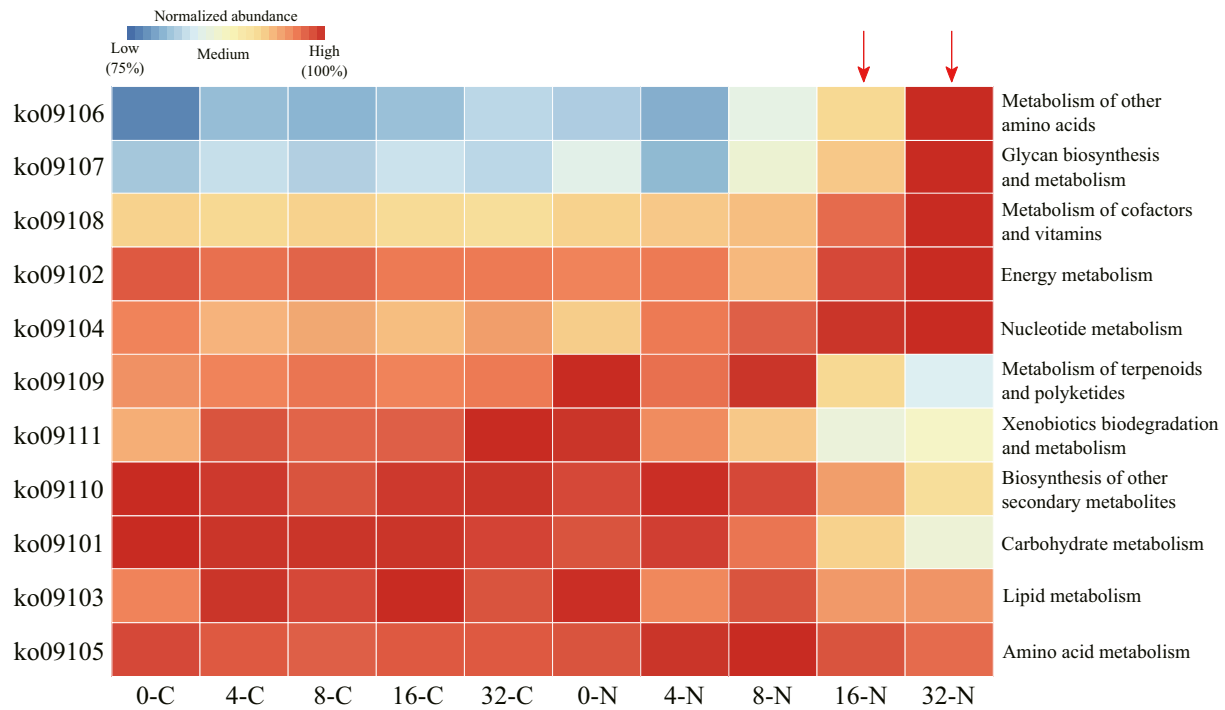


**Fig. 4.** Predictive metabolic profiling, based on KEGG orthology (ko) Level 2. The late nitrate communities (16-N and 32-N) were significantly different from the others, as seen from the enhanced metabolisms of other amino acids, glycan, nucleotide, cofactors and vitamins, and seen from the suppressed expression in terpenoids, polyketides, xenobiotics, lipid and carbohydrate.

suggested the competent metabolic fitness of *Thiobacillus*. Linear regression also identified positive correlations between its relative abundance and nitrate consumption, nitrite production and sulfate production (Fig. 5B–D).

Community enrichments of different dilutabilities were streaked on NS and NTS plates (anaerobic, room temperature). However, no colony formed on the NS plates. Using solid NTS medium, 14 strains were isolated and all were members of the phylum *Proteobacteria* (Table 1).

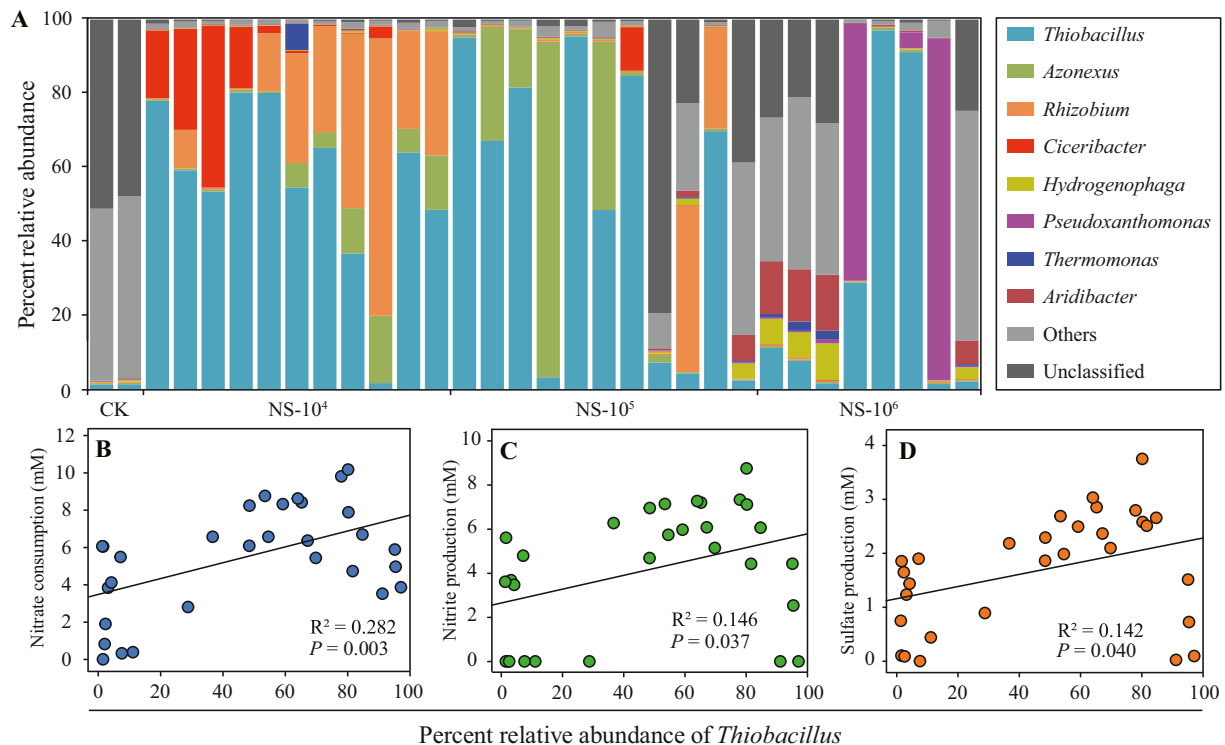


**Fig. 5.** *Thiobacillus* became the best competitor in diluted communities. (A) Community compositions of diluted then enriched communities at the genus level. CK – control communities; NS – the medium, followed by the dilution factors. (B), (C) and (D) – linear fitting for *Thiobacillus* relative abundance versus nitrate consumption, nitrite production and sulfate production.

**Table 1**

Strains isolated from enriched sediment communities on NTS plates.

Train	Closest relative	Identity	Class of Proteobacteria	GenBank accession	Nitrate reduction	Sulfide oxidation	Thiosulfate oxidation	narG	napA	nirK/S	soxB
F21	<i>Ciceribacter thiooxidans</i>	99.9%	α	KU985322	(+)	(-)	(+)	(+)	(-)	K	(+)
T6647	<i>Aminobacter niigataensis</i>	99.3%	α	MT568546	(+)	(-)	(+)	(+)	(-)	K	(-)
T677	<i>Afpia felis</i>	97.4%	α	MT568547	(+)	(-)	(+)	(+)	(+)	K	(+)
T681	<i>Bosea robiniae</i>	98.9%	α	MT568548	(+)	(-)	(+)	(+)	(+)	K	(-)
T83	<i>Sphingopyxis terrae</i>	99.8%	α	MT568549	(+)	(-)	(+)	(-)	(-)	S	(-)
T5712	<i>Achromobacter insuavis</i>	99.4%	β	MT568550	(+)	(-)	(+)	(+)	(+)	K	(-)
S5643	<i>Thiobacillus thiophilus</i>	98.4%	β	MT568551	(+)	(+)	(+)	(+)	(+)	S	(+)
S544	<i>Azonexus caeni</i>	99.5%	β	MT568552	(+)	(-)	(+)	(-)	(+)	S	(+)
T84	<i>Hydrogenophaga intermedia</i>	99.0%	β	MT568553	(+)	(-)	(+)	(+)	(-)	S	(+)
T572	<i>Alicyclophilus denitrificans</i>	99.6%	β	MT568554	(+)	(-)	(+)	(+)	(-)	S	(+)
T763	<i>Pseudomonas stutzeri</i>	99.2%	γ	MT568555	(+)	(-)	(+)	(+)	(+)	S	(-)
T568	<i>Thermomonas koreensis</i>	99.9%	γ	MT568556	(+)	(-)	(+)	(+)	(-)	KS	(-)
S685	<i>Pseudoxanthomonas mexicana</i>	99.4%	γ	MT568557	(+)	(-)	(+)	(-)	(+)	K	(-)
T546	<i>Rhodanobacter lindaniclasticus</i>	99.6%	γ	MT568558	(+)	(-)	(+)	(-)	(-)	K	(-)

Unlike community enrichments, these pure isolates were proved able to oxidize thiosulfate and reduce nitrate since interspecific cross-feeding was excluded. We then determined their metabolic characteristics using liquid NS and NTS medium, and found that strain S5643 (*Thiobacillus thiophilus*) was the sole sulfide oxidizer. PCR of selected functional genes involved in nitrogen and sulfur cycling found that (i) all strains except T83 (*Sphingopyxis terrae*) and T546 (*Rhodanobacter lindaniclasticus*) had nitrate reductase *narG* or *napA*; (ii) all strains harbored nitrite reductase *nirK* or *nirS*; and (iii) thiosulfate oxidase *soxB* appeared only in 6 strains (Table 1), including S5643. These results confirmed the metabolic fitness of *Thiobacillus*, which was the sole sulfide-oxidizing denitrifier among the 14 isolates.

### 3. Discussion

Patterns of microbial community assembly and interaction in river sediments are far from clear, evidenced by the high proportion of uncultured and unclassified organisms present in subsurface environments together with the overwhelming discovery of new microbial lineages involved in major geochemical cycles (Anantharaman et al., 2016). In this study, we showed that nitrate amendment to sulfide-rich river sediments overwrote the redox conditions and thus simplified the microbial community composition and interaction by enriching two sulfur-oxidizing denitrifiers.

Most denitrifiers are heterotrophs and a minor group are chemoautotrophs that utilize inorganic energy sources such as reduced sulfur and Fe(II) (Hayakawa et al., 2013). After nitrate amendment, we identified (i) a consistent nitrate reduction and the coupled AVS oxidation, (ii) an accumulation of nitrite and sulfate, and (iii) a drastic Fe(II) oxidation and the coupled Fe(III) accumulation in the final stage (Fig. S6). Notably, more nitrate in stoichiometry was consumed than the sum consumption of AVS and Fe(II) if N<sub>2</sub> was the end product (by denitrification), so there must have been cryptic electron donors fueling nitrate reduction (see supplementary information: the cryptic electron donor).

Among the identified genera, the control and early nitrate communities were dominated by methanogens (Braeuer et al., 2011; Imachi et al., 2008; Kroeninger et al., 2017; Ma et al., 2005; Patel and Sprott, 1990) and syntrophic bacteria (de Bok et al., 2001; McInerney et al., 2007; Qiu et al., 2008). When exposed to elevated nitrate, most genera were gradually outcompeted including some denitrifiers. Members of *Thiobacillus* were characterized as autotrophic sulfide oxidizers and denitrifiers (Bosch et al., 2012; Dolejs et al., 2015); *T. ferrooxidans* might even feed on Fe(II) (Nemati et al., 1998). The *Thiobacillus* detected from late nitrate communities shared the highest 16S rRNA gene

similarity with *T. thiophilus* strain D24TN (99%) and *T. denitrificans* strain NCIMB 9548 (98%), both were obligate chemolithotrophs and facultative anaerobes, using thiosulfate or AVS as the electron donor, nitrate or oxygen as the electron acceptor, and CO<sub>2</sub> as the sole carbon source (Kellermann and Griebler, 2009; Kelly and Wood, 2000).

The dominance of *Thiobacillus* (in abundance) reappeared in the community enrichments (Figs. 2E, 5A). Moreover, pure culture of isolated *T. thiophilus* was performing simultaneous nitrate-reduction, AVS-oxidation and thiosulfate-oxidation (Table 1) so that it dominated NS enrichments (in abundance) because of its high metabolic fitness. Consistently, several studies identified an enhanced sulfide oxidation alongside the rise of *Thiobacillus* after nitrate amendment (He et al., 2018, 2017; Xu et al., 2014). The other winner *Luteimonas*, was barely detectable at first but significantly enriched later on, in agreement with a recent discovery in which *Luteimonas* dominated communities of sediment samples with an increasing proportion of recalcitrant carbon (Wu et al., 2018). *Luteimonas* spp. might be a potential Fe(II) oxidizer, as Zhang et al. identified a predicted ferric reductase gene and two subunits of ferredoxin nitrite reductase from the genome of *L. abyssi* XH301<sup>T</sup> (Zhang et al., 2015).

There are studies pointing out that community functionality is a direct reflection of physiochemical condition (Gibbons, 2017; Louca et al., 2017; Nelson et al., 2016), and the rise of *Luteimonas* and *Thiobacillus* well substantiated that. Among so many denitrifiers, why lithotrophic *Luteimonas* and *Thiobacillus* rather than those organotrophs gained dominance remained unclear, in the presence of so abundant TOC.

Keystone taxa are believed important in maintaining the functionality and integrity of an ecosystem, whose extinction often leads to community fragmentation or even collapse (Wu et al., 2016). In this study, microbial covariation networks under nitrate pollution were getting simpler along with the loss of keystone taxa which predominantly comprised of members of Class *Proteobacteria* and *Chloroflexi*, as hypothesized. We identified no strong correlation between OTU abundances and their network connectivity, although keystone nodes turned to be sparse OTUs. Instead, the network connectivity was speculated highly associated with metabolic behavior of individual OTUs, such as cross-feedings or metabolic interdependencies that were predominantly sustained by native auxotrophs (Embree et al., 2015; Hubalek et al., 2017; Mee et al., 2014; Ponomarova and Patil, 2015). For example, syntrophic bacteria (e.g. *Smithella* and *Syntrophorhabdus*) and methanogens (e.g. *Methanolinea*) were auxotrophs, performing extensive interspecific cross-feeding, and were keystone taxa in the microbial covariation networks. In addition, several studies confirmed the auxotrophic metabolisms between auxotrophs and methanogens (Heyer et al., 2019; Wawrik et al., 2016; Zhu et al., 2020).

Nitrate amendment might have other effects on microbial communities than simplification. We identified several rapid microbial responses to elevated nitrate, whereas the community richness,  $\alpha$ -diversity and evenness were little affected (Fig. 2, Day 0–4). Several genera such as *Methanomassiliicoccus*, *Vulcanibacillus*, *Thermomonas* and *Bacillus* were significantly enriched on Day 4 but were eventually suppressed or eliminated (Fig. 1E, F). So elevated nitrate introduced both days- and weeks-effects upon microbial communities of sulfide-rich river sediment. For the first few days it boosted biodiversity possibly by niche creation (e.g. bridging metabolic interdependencies between nitrate reducers and AVS oxidizers), in agreement with our previous work (Xu et al., 2014).

#### 4. Conclusions

This study provides insights into microbial assemblage and interactions in river sediments when microorganisms were exposed to nitrate pollution. Microbial communities were simplified and specialized in nitrate reduction coupled with sulfide and Fe(II) oxidation. *Thiobacillus* and *Luteimonas* gained dominance alongside the elimination of keystone taxa, leading to fragmented covariation networks. The significant loss of biodiversity and other functions was considered a negative ecological impact of nitrate amendment on the microbial community of river sediments. We recommend considering the effects of nitrate amendment to native auxotrophs before its application.

#### 5. Material and methods

##### 5.1. Experiment design and sample process

River surface sediments (0–10 cm in depth) from the Pearl River Delta (22°14'50" N, 113°11'50" E) were sampled in December 2017. Plant residues, macrofauna and large particles were removed by hand grubbing. The resulting sediment was vigorously homogenized and distributed to 40 g (wet weight) per share. Sterilized pure water with or without ~7.74 mM calcium nitrate was added to the sediments, making each tube to the volume of 45 ml. In sum, we prepared 60 tubes with nitrate (as treatment) and 60 without nitrate (as control). All tubes were anaerobically cultured at room temperature. 12 treatment and 12 control tubes were collected on Day 0, 4, 8, 16, 32 respectively for physiochemical characterizations and DNA extraction. We quantified the levels of AVS, ferrous iron, total iron, pH, nitrate, nitrite, sulfate, and TOC (total organic carbon). See supplementary information for detailed measurements. For convenience, we assigned all 120 samples into two groups: Nitrate and Control, 60 samples each. Each group had five subgroups based on sampling time, i.e. 0-N, 4-N, 8-N, 16-N, and 32-N for nitrate group, while 0-C, 4-C, 8-C, 16-C and 32-C for control. Each subgroup consisted of 12 replicates.

To analyze the composition of nitrate-reducing sulfur-oxidizing bacteria (NR-SOB) in the sediment, a group of serial dilution enrichments (Lagier et al., 2018) with 12 series repetitions were prepared in medium NS (nitrate as the sole electron acceptor and sulfide as the sole electron donor). See supplementary information for medium chemical compositions. 1 g wet sediment (~80% w/w water content) was added to 9 ml medium to get the  $10^1$  dilution factor. The serial dilution was conducted every ten-fold until  $10^{-8}$ . Enrichments at each dilution factor had 12 parallels. Note that parallels here were not equivalent to replicates since every dilution was random so that the resulting community compositions might differ. See supplementary information for sample cultivation. All samples were quantified of nitrate consumption to roughly represent metabolic intensity. The resulting NR-SOB strains were isolated by plate-streaking on medium NTS (thiosulfate as the sole electron donor) plates supplemented with 1.5% agar respectively. After one-month anaerobic cultivation, different colonies were isolated, purified and identified by colony PCR of full length 16S rRNA gene.

##### 5.2. Illumina Miseq sequencing and predictive functional profiling

Sequencing of 16S ribosome RNA gene V4 region was used to track community successions. Qualified DNA libraries were sequenced and clustered into de novo OTUs by the Usearch (v9.2.64) pipeline (Edgar, 2010). See supplementary information for detailed sequence processing. Briefly, each sample was rarefied to 10,000 clean reads. Sequencing of 16S rRNA gene gives no direct metabolic information so we used FAPROTAX (Louca et al., 2016) and PICRUSt (Langille et al., 2013) just to roughly estimate the functional changes under nitrate stimulation. Clean 16S rRNA gene tags were re-clustered against the GreenGenes database (v13.8, 97\_otus.fasta) to be compatible with FAPROTAX (v1.1) and PICRUSt (v1.1.1). FAPROTAX was used to identify putative functional microbial members, and PICRUSt was to compare the gene abundance before and after nitrate stimulation, especially those involved in N or S metabolisms. Both predictions were based on the same normalized closed-reference OTU table. We also employed DADA2, the state-of-art analytical tool to re-analysis the community composition. The resulting community compositions were highly similar to those constructed by the Usearch pipeline (Fig. S7 and Table S4). See supplementary information for detailed comparison.

##### 5.3. Covariation network construction and visualization

Each network was constructed based on Spearman's correlation coefficient of the 12 replicates by the MENA pipeline (<http://ieg4.rccc.ou.edu/MENA/>) (Deng et al., 2012; Zhou et al., 2010, 2011), yielding 10 networks. In network construction, the threshold was automatically determined in the Random Mateix Theory-based modeling. Only OTUs present in more than 8 out of 12 replicates were involved. Output networks were visualized using Gephi (v0.9.2). A visualized covariation network consisted of nodes and links. A node represented an OTU that had significant Spearman's correlations (above the network threshold) with other nodes. A link between two nodes represented their negative or positive covariation (Bascompte, 2007; Montoya et al., 2006) depend on the calculated correlation coefficient ( $-1$  to  $+1$ ). A positive correlation meant the two nodes were sharing a same changing pattern. A module referred to a group of nodes that were highly interconnected within the group and had fewer or no connections outside the group. MENA has four built-in methods for module separation, and we selected the greedy modularity optimization because it generated the highest Modularity index ( $M$ ). Generally, the number of nodes defines the network size, while the numbers of modules and links per node define the network complexity. See supplementary information for the classification of peripherals, module hubs, connectors and network hubs.

##### 5.4. Statistical analysis

Shannon's index ( $H$ ) and Simpson's evenness ( $J$ ) were calculated to represent alpha-diversity of each community. Community dissimilarity between control and nitrate group was compared using PCoA and one-way ANOSIM, both were based on Bray-Curtis distance. Genera that significantly changed in relative abundance over time or over treatment were selected. We confirmed the compliance of normal distribution of genus frequencies and then quantified the dissimilarities by one-way  $t$ -test. Alpha-diversity, PCoA and ANOSIM were performed with R (Vegan package, v2.4-6) (Oksanen et al., 2010).

Supplementary data to this article can be found online at <https://doi.org/10.1016/j.scitotenv.2020.141513>.

#### Funding

This work was funded by:

- National Natural Science Foundation of China (91851202, 51678163, U1701243, 91951207)

- GDAS' Special Project of Science and Technology Development (2019GDASYL-0104005, 2020GDASYL-20200402001)
- Guangdong Provincial Programs for Science and Technology Development (2018B030324002, 2019B110205004)
- Science and Technology Project of Guangzhou (201707020021).

## Data availability

Raw Illumina reads of the 16S ribosomal RNA gene used to track community successions and to construct microbial interactive networks are available in the NCBI SRA. BioProject: Ronggui-sediment, Accession: PRJNA526396 (<https://www.ncbi.nlm.nih.gov/sra/?term=PRJNA526396>). The full-length 16S rRNA gene sequences of 14 isolates are available in the NCBI GenBank, accession: KU985322, MT568546-MT568558.

## CRediT authorship contribution statement

**Enze Li:** Conceptualization, Formal analysis, Writing - original draft, Writing - review & editing. **Tongchu Deng:** Conceptualization, Investigation, Formal analysis, Writing - review & editing. **Lei Yan:** Conceptualization, Investigation, Writing - review & editing. **Jizhong Zhou:** Conceptualization, Writing - original draft, Writing - review & editing. **Zhili He:** Conceptualization, Writing - original draft, Writing - review & editing. **Ye Deng:** Conceptualization, Writing - original draft, Writing - review & editing. **Meiying Xu:** Conceptualization, Methodology, Writing - original draft, Writing - review & editing.

## Declaration of competing interest

The authors declare that they have no known competing financial interests or personal relationships that could have appeared to influence the work reported in this paper.

## References

- Anantharaman, K., Brown, C.T., Hug, L.A., Sharon, I., Castelle, C.J., Probst, A.J., et al., 2016. Thousands of microbial genomes shed light on interconnected biogeochemical processes in an aquifer system. *Nat. Commun.* 7.
- Bascompte, J., 2007. Networks in ecology. *Basic Appl. Ecol.* 8, 485–490.
- de Bok, F.A.M., Stams, A.J.M., Dijkema, C., Boone, D.R., 2001. Pathway of propionate oxidation by a syntrophic culture of *Smithella propionica* and *Methanospirillum hungatei*. *Appl. Environ. Microbiol.* 67, 1800–1804.
- Bosch, J., Lee, K.-Y., Jordan, G., Kim, K.-W., Meckenstock, R.U., 2012. Anaerobic, nitrate-dependent oxidation of pyrite nanoparticles by *Thiobacillus denitrificans*. *Environ. Sci. Technol.* 46, 2095–2101.
- Brauer, S.L., Cadillo-Quiroz, H., Ward, R.J., Yavitt, J.B., Zinder, S.H., 2011. *Methanoregula boonei* gen. nov., sp. nov., an acidiphilic methanogen isolated from an acidic peat bog. *Int. J. Syst. Evol. Microbiol.* 61, 45–52.
- Burgin, A.J., Hamilton, S.K., 2007. Have we overemphasized the role of denitrification in aquatic ecosystems? A review of nitrate removal pathways. *Front. Ecol. Environ.* 5, 89–96.
- Cheng, F.Y., Basu, N.B., 2017. Biogeochemical hotspots: role of small water bodies in landscape nutrient processing. *Water Resour. Res.* 53, 5038–5056.
- Deng, Y., Jiang, Y.-H., Yang, Y., He, Z., Luo, F., Zhou, J., 2012. Molecular ecological network analyses. *BMC Bioinforma.* 13.
- Dolejs, P., Paclík, L., Maca, J., Pokorna, D., Zabranska, J., Bartacek, J., 2015. Effect of S/N ratio on sulfide removal by autotrophic denitrification. *Appl. Microbiol. Biotechnol.* 99, 2383–2392.
- Donaldson, G.P., Lee, S.M., Mazmanian, S.K., 2016. Gut biogeography of the bacterial microbiota. *Nat. Rev. Microbiol.* 14, 20–32.
- Edgar, R.C., 2010. Search and clustering orders of magnitude faster than BLAST. *Bioinformatics* 26, 2460–2461.
- Embree, M., Liu, J.K., Al-Bassam, M.M., Zengler, K., 2015. Networks of energetic and metabolic interactions define dynamics in microbial communities. *Proc. Natl. Acad. Sci. U. S. A.* 112, 15450–15455.
- Evans, S., Martiny, J.B., Allison, S.D., 2017. Effects of dispersal and selection on stochastic assembly in microbial communities. *ISME J.* 11, 176.
- Falkowski, P.G., Fenchel, T., DeLong, E.F., 2008. The microbial engines that drive Earth's biogeochemical cycles. *science* 320, 1034–1039.
- Gibbons, S.M., 2017. Microbial community ecology function over phylogeny. *Nat. Ecol. Evol.* 1.
- Griffiths, B.S., Philippot, L., 2013. Insights into the resistance and resilience of the soil microbial community. *FEMS Microbiol. Rev.* 37, 112–129.
- Hayakawa, A., Hatakeyama, M., Asano, R., Ishikawa, Y., Hidaka, S., 2013. Nitrate reduction coupled with pyrite oxidation in the surface sediments of a sulfide-rich ecosystem. *J. Geophys. Res. Biogeosci.* 118, 639–649.
- He, Z., Long, X., Li, L., Yu, G., Chong, Y., Xing, W., et al., 2017. Temperature response of sulfide/ferrous oxidation and microbial community in anoxic sediments treated with calcium nitrate addition. *J. Environ. Manag.* 191, 209–218.
- He, Z., Huang, R., Liang, Y., Yu, G., Chong, Y., Wang, L., 2018. Index for nitrate dosage calculation on sediment odor control using nitrate-dependent ferrous and sulfide oxidation interactions. *J. Environ. Manag.* 226, 289–297.
- Heyer, R., Schallert, K., Siewert, C., Kohrs, F., Greve, J., Maus, I., et al., 2019. Metaproteome analysis reveals that syntrophy, competition, and phage-host interaction shape microbial communities in biogas plants. *Microbiome* 7.
- Hubalek, V., Buck, M., Tan, B., Foght, J., Wendeberg, A., Berry, D., et al., 2017. Vitamin and amino acid auxotrophy in anaerobic consortia operating under methanogenic conditions. *Msystems* 2.
- Imachi, H., Sakai, S., Sekiguchi, Y., Hanada, S., Kamagata, Y., Ohashi, A., et al., 2008. *Methanolinea tarda* gen. nov., sp. nov., a methane-producing archaeon isolated from a methanogenic digester sludge. *Int. J. Syst. Evol. Microbiol.* 58, 294–301.
- Isbell, F., Craven, D., Connolly, J., Loreau, M., Schmid, B., Beierkuhnlein, C., et al., 2015. Biodiversity increases the resistance of ecosystem productivity to climate extremes. *Nature* 526, 574.
- Kazakis, N., Matiatos, L., Ntona, M.M., Bannenberg, M., Kalaitzidou, K., Kaprara, E., et al., 2020. Origin, implications and management strategies for nitrate pollution in surface and ground waters of Anthemountas basin based on a delta N-15-NO3- and delta O-18-NO3- isotope approach. *Sci. Total Environ.* 724.
- Kellermann, C., Griebler, C., 2009. *Thiobacillus thiophilus* sp. nov., a chemolithoautotrophic, thiosulfate-oxidizing bacterium isolated from contaminated aquifer sediments. *Int. J. Syst. Evol. Microbiol.* 59, 583–588.
- Kelly, D.P., Wood, A.P., 2000. Confirmation of *Thiobacillus denitrificans* as a species of the genus *Thiobacillus*, in the beta-subclass of the Proteobacteria, with strain NCIMB 9548 as the type strain. *Int. J. Syst. Evol. Microbiol.* 50, 547–550.
- Kroeninger, L., Gottschling, J., Deppenmeier, U., 2017. Growth characteristics of *Methanomassiliococcus luminyensis* and expression of methyltransferase encoding genes. *Archaea* 2017, 2756573.
- Lagier, J.-C., Dubourg, G., Million, M., Cadoret, F., Bilen, M., Fenollar, F., et al., 2018. Culturing the human microbiota and culturomics. *Nat. Rev. Microbiol.* 16, 540–550.
- Langille, M.G.I., Zaneveld, J., Caporaso, J.G., McDonald, D., Knights, D., Reyes, J.A., et al., 2013. Predictive functional profiling of microbial communities using 16S rRNA marker gene sequences. *Nat. Biotechnol.* 31, 814.
- Lee, S.-H., Park, J.-H., Kim, S.-H., Yu, B.J., Yoon, J.-J., Park, H.-D., 2015. Evidence of syntrophic acetate oxidation by Spirochaetes during anaerobic methane production. *Bioresour. Technol.* 190, 543–549.
- Louca, S., Parfrey, L.W., Doebeli, M., 2016. Decoupling function and taxonomy in the global ocean microbiome. *Science* 353, 1272–1277.
- Louca, S., Jacques, S.M.S., Pires, A.P.F., Leal, J.S., Srivastava, D.S., Parfrey, L.W., et al., 2017. High taxonomic variability despite stable functional structure across microbial communities. *Nat. Ecol. Evol.* 1.
- Ma, K., Liu, X.L., Dong, X.Z., 2005. *Methanobacterium beijingense* sp. nov., a novel methanogen isolated from anaerobic digesters. *Int. J. Syst. Evol. Microbiol.* 55, 325–329.
- McInerney, M.J., Rohlin, L., Mouttaki, H., Kim, U., Krupp, R.S., Rios-Hernandez, L., et al., 2007. The genome of *Syntrophus aciditrophicus*: life at the thermodynamic limit of microbial growth. *Proc. Natl. Acad. Sci. U. S. A.* 104, 7600–7605.
- Mee, M.T., Collins, J.J., Church, G.M., Wang, H.H., 2014. Syntrophic exchange in synthetic microbial communities. *Proc. Natl. Acad. Sci. U. S. A.* 111, E2149–E2156.
- Montoya, J.M., Pimm, S.L., Solé, R.V., 2006. Ecological networks and their fragility. *Nature* 442, 259.
- Nelson, M.B., Martiny, A.C., Martiny, J.B.H., 2016. Global biogeography of microbial nitrogen-cycling traits in soil. *Proc. Natl. Acad. Sci. U. S. A.* 113, 8033–8040.
- Nemati, M., Harrison, S.T.L., Hansford, G.S., Webb, C., 1998. Biological oxidation of ferrous sulphate by *Thiobacillus ferrooxidans*: a review on the kinetic aspects. *Biochem. Eng. J.* 1, 171–190.
- Oksanen, J., Blanchet, F.G., Kindt, R., Legendre, P., O'hara, R.B., Simpson, G.L., et al., . Vegan: Community Ecology Package. R Package Version 1.17-4 (<http://cran.r-project.org> (Accessed em 2010)).
- Patel, G.B., Sprott, G.D., 1990. *Methanoseta concilii* gen-nov, sp-nov (*Methanohalobium concilii*) and *Methanoseta thermoacetophila* nom-rev, comb-nov. *Int. J. Syst. Bacteriol.* 40, 79–82.
- Ponomarova, O., Patil, K.R., 2015. Metabolic interactions in microbial communities: untangling the Gordian knot. *Curr. Opin. Microbiol.* 27, 37–44.
- Qiu, Y.-L., Hanada, S., Ohashi, A., Harada, H., Kamagata, Y., Sekiguchi, Y., 2008. *Syntrophorhabdus aromaticivorans* gen. nov., sp. nov., the first cultured anaerobe capable of degrading phenol to acetate in obligate syntrophic associations with a hydrogenotrophic methanogen. *Appl. Environ. Microbiol.* 74, 2051–2058.
- Shang, X., Huang, H., Mei, K., Xia, F., Chen, Z., Yang, Y., et al., 2020. Riverine nitrate source apportionment using dual stable isotopes in a drinking water source watershed of Southeast China. *Sci. Total Environ.* 724.
- Wawrik, B., Marks, C.R., Davidova, I.A., McInerney, M.J., Pruitt, S., Duncan, K.E., et al., 2016. Methanogenic paraffin degradation proceeds via alkane addition to fumarate by *Smithella* spp. mediated by a syntrophic coupling with hydrogenotrophic methanogens. *Environ. Microbiol.* 18, 2604–2619.
- Wu, J.H., Sun, Z.C., 2016. Evaluation of shallow groundwater contamination and associated human health risk in an alluvial plain impacted by agricultural and industrial activities, Mid-west China. *Exposure Health* 8, 311–329.

- Wu, L., Yang, Y., Chen, S., Zhao, M., Zhu, Z., Yang, S., et al., 2016. Long-term successional dynamics of microbial association networks in anaerobic digestion processes. *Water Res.* 104, 1–10.
- Wu, X., Wu, L., Liu, Y., Zhang, P., Li, Q., Zhou, J., et al., 2018. Microbial interactions with dissolved organic matter drive carbon dynamics and community succession. *Front. Microbiol.* 9.
- Xia, X.H., Zhang, S.B., Li, S.L., Zhang, L.W., Wang, G.Q., Zhang, L., et al., 2018. The cycle of nitrogen in river systems: sources, transformation, and flux. *Environ. Sci. Process. Impacts* 20, 863–891.
- Xu, M., Zhang, Q., Xia, C., Zhong, Y., Sun, G., Guo, J., et al., 2014. Elevated nitrate enriches microbial functional genes for potential bioremediation of complexly contaminated sediments. *ISME J.* 8, 1932.
- Xun, W., Li, W., Xiong, W., Ren, Y., Liu, Y., Miao, Y., et al., 2019. Diversity-triggered deterministic bacterial assembly constrains community functions. *Nat. Commun.* 10.
- Zhang, L., Wang, X., Yu, M., Qiao, Y., Zhang, X.-H., 2015. Genomic analysis of *Luteimonas abyssi* XH031(T): insights into its adaption to the subseafloor environment of South Pacific Gyre and ecological role in biogeochemical cycle. *BMC Genomics* 16.
- Zhou, J., Deng, Y., Luo, F., He, Z., Tu, Q., Zhi, X., 2010. Functional molecular ecological networks. *Mbio* 1.
- Zhou, J., Deng, Y., Luo, F., He, Z., Yang, Y., 2011. Phylogenetic molecular ecological network of soil microbial communities in response to elevated CO<sub>2</sub>. *Mbio* 2.
- Zhu, X.Y., Campanaro, S., Treu, L., Seshadri, R., Ivanova, N., Kougias, P.G., et al., 2020. Metabolic dependencies govern microbial syntrophies during methanogenesis in an anaerobic digestion ecosystem. *Microbiome* 8.

# Supplementary information of

## Elevated Nitrate Simplifies Microbial Community Compositions and Interactions in Sulfide-rich River Sediments

**Sediment chemical measurements.** Sediments were fully resuspended in an anaerobic workstation and were centrifuged ( $10000\times g$ , 5 min) to remove solids. Supernatant passed through a  $0.22\ \mu\text{m}$  filter. Both solids and effluents were kept. Nitrate, nitrite and sulfate were retained in the effluents and were quantified using ion chromatography (Dionex ICS-1100, Thermofisher, USA). Total organic carbon (TOC), total acid-soluble iron (T-Fe) and AVS existed in both solids and effluents. TOC was measured using a TOC analyzer (TOC-L, SHIMADZU, Japan). AVS and T-Fe were measured using the methods reported by Allen et al. (Allen, Fu, & Deng, 1993).

**DNA extraction and purification.** 12 sediment replicates (10 g, wet weight) of each treatment were mixed with 10 mL phosphate buffer (2.70 mM KCl, 137 mM NaCl, 4.30 mM  $\text{Na}_2\text{HPO}_4$  and 1.40 mM  $\text{KH}_2\text{PO}_4$ ; pH 7.3) and were vortexed for 20 min, cells harvested by centrifugation at  $8,000\times g$ , 10 min. The community genomic DNA was extracted from cell pellets using PowerSoil DNA isolation kit (MO BIO Laboratories, USA) according to the manufacturer's instruction. The double-barcoded universal primer set 515F (5'-GTG CCA GCM GCCGCG GTA A-3') and 806R (5'-GGACTACHVGGGTWTCTAAT-3') was used to amplify the V4 hypervariable region. PCR mixture (50  $\mu\text{l}$ ) contained 20 ng gDNA, 5  $\mu\text{l}$   $10\times$  EasyPCR buffer (TransGen, China), F/R primer at 0.5  $\mu\text{M}$ , each dNTP at 20  $\mu\text{M}$  and 2.5 U of EasyTaq DNA Polymerase (TransGen, China). PCR program included an initial denaturation (94 °C, 1 min), 30 cycles of 94 °C for 20 s, 57 °C for 25 s and 68 °C for 45 s, and a final extension (68 °C, 10 min). PCR products were purified via gel electrophoresis and gel extraction.

**Miseq sequencing.** The library was constructed with VAHTS<sup>TM</sup> Nano DNA Library Prep Kit for Illumina (Vazyme Biotech Co.,Ltd, China). Clean reads were analyzed by the Usearch pipeline (v9.2.64). Sequences having any of the below conditions were discarded: (a) unidentifiable barcode or primer ( $>3$  base errors); (b) one or more N bases; (c) out of 240 to 260 bp in length; (d) any base with a Q-score below 20. In the Uparse clustering (Edgar, 2013), chimeric sequences were automatically removed and a *de novo* OTU table was constructed at a 97% cutoff. Singletons were removed too. The taxonomic assignment of each OTU was performed with the RDP classifier v2.12 (Wang, Garrity, Tiedje, & Cole, 2007) at a confidence of 0.7.

### About batch effects

The whole experiment involved only two batches of sequencing, once for all control samples and once for all nitrate treatments. Every time when an incubation was over, the sediments were frozen until all incubations were complete on Day 32. Genome extraction occurred twice as well, once for all control samples and once for all nitrate treatments. Though batch effects were inevitable (Gibbons, Duvall, & Alm, 2018), we did what we could to minimize them, for example, the identical sample processing procedure, identical library construction kit, identical sequencing platform (MiSeq) and identical NGS pipeline.

### Enrichment serial dilution, strain isolation and identification of NR-SOB

Two groups of serial dilution were performed using medium NS and medium NTS, respectively. Medium NS contained 1 g/L KNO<sub>3</sub>, 1 g/L Na<sub>2</sub>S·9H<sub>2</sub>O, 1 g/L NaHCO<sub>3</sub>, 0.5 g/L FeCl<sub>2</sub>, 2g/L KH<sub>2</sub>PO<sub>4</sub> and 0.1g/L MgCl<sub>2</sub>. Medium NTS contained 1 g/L KNO<sub>3</sub>, 2 g/L Na<sub>2</sub>S<sub>2</sub>O<sub>3</sub>·6H<sub>2</sub>O, 1 g/L NaHCO<sub>3</sub>, 2g/L KH<sub>2</sub>PO<sub>4</sub> and 0.1g/L MgCl<sub>2</sub>. Samples were statically and anaerobically cultivated for 30 days. The entire incubation lasted for 90 days and included two transfers on Day 30 and 60 respectively, to fresh NS/NTS media to obtain stable enrichments. During the second transfer, equal biomass of each enrichment was sampled and monitored of NO<sub>3</sub><sup>-</sup>, NO<sub>2</sub><sup>-</sup>, SO<sub>4</sub><sup>2-</sup> and S<sub>2</sub>O<sub>3</sub><sup>2-</sup> by ion chromatography to estimate the metabolic intensity (ThermoFisher Scientific Ion Chromatography ICS-1100 equipped with a AS-25 column). Strains of NR-SOB were isolated by dilution-plate method in NS and NTS media supplemented with 1.5% agar. After one-month anaerobic cultivation, different strains were picked and purified by consecutive plate streaking.

**Interactive network visualization.** In Gephi, we selected Fruchterman Reingold (Fruchterman & Reingold, 1991) and Yifan Hu layouts (Hu & Shi, 2014) to visualize the networks. In Fruchterman Reingold layout, node size was proportional to its degree (sum of in- and out-degree) to underline individual topological significance (Figure 3). Modules consisting of over 5 nodes were randomly colored, the rest left grey. Nodes of a same module were gathered close to each other. Links were classified either positive (+1) or negative (-1) based on Spearman’s correlation coefficient; the former were colored green and the latter were colored red. Yifan Hu layout focused on the among-module connectivity, where the interconnected nodes were packed closer to each other. Major modules (≥ 5 nodes) were randomly colored as well and the links within shared the same coloration.

**Table S1. Statistics of networks.**

Timepoint	Control					Nitrate				
	Day 0	Day 4	Day 8	Day 16	Day 32	Day 0	Day 4	Day 8	Day 16	Day 32
Similarity Threshold	0.800	0.810	0.820	0.820	0.810	0.800	0.780	0.770	0.780	0.760
Network Size (No. Nodes)	436	472	416	414	406	308	336	280	190	94
Covariation (No. Links)	560	560	607	627	540	590	434	349	317	87
Positive Links	50.1%	56.6%	49.6%	48.2%	47.2%	74.8%	80.97%	80.5%	93.7%	95.4%
No. Modules	48	52	49	47	45	45	44	32	28	25
No. Major Modules <sup>a</sup>	19	16	15	16	18	13	13	13	8	5
Modularity <sup>b</sup>	0.838	0.793	0.654	0.739	0.832	0.649	0.842	0.848	0.740	0.805
Average Degree <sup>c</sup>	2.569	3.067	3.880	3.126	2.660	4.012	2.583	2.493	3.337	1.851

<sup>a</sup> A module consists of more than 5 interconnected nodes and is therefore considered important in scaffolding an interactive network.

<sup>b</sup> Modularity defines how well a network is separated into modules <sup>6</sup>.

<sup>c</sup>  $\frac{\sum_{i=1}^n k_i}{n}$ , where  $k_i$  is the degree of node  $i$ ,  $n$  is the network size, i.e. number of nodes. Higher average degree means a

network with greater density of covariations.

**Node connectivity and putative keystone nodes.** Node connectivity is an indicator of topological significance in networks. Each node has several parameters to define its connectivity. Those of great connectivity are referred to as keystone nodes, which may scaffold a module and/or connect to several modules (Guimera, Sales-Pardo, & Amaral, 2007). We selected  $ZP$  values (Guimera & Amaral, 2005) to compare the connectivity of nodes of different networks.  $ZP$  values stood for the within-module ( $Z_i$ ) and among-module connectivity ( $P_i$ ) of each node. According to Deng et al,  $ZP$  plot was divided into four quadrants, (i) the peripherals ( $Z_i \leq 2.5, P_i \leq 0.62$ ) having no significantly topological roles in the network; (ii) the connectors ( $Z_i \leq 2.5, P_i > 0.62$ ) significant in connecting modules; (iii) the module hubs ( $Z_i > 2.5, P_i \leq 0.62$ ) that scaffolded their own modules, and (iv) the network hubs ( $Z_i > 2.5$  and  $P_i > 0.62$ ), which acted as both connectors and module hubs. Connectors, module hubs and network hubs were putative keystone nodes; their corresponding taxa were thus putative keystone taxa.

$ZP$  values of all nodes were plotted in Figure S2A. A node/OTU present in several networks might be plotted more than once if they had different  $ZP$  values in different networks. Of all the 3352 nodes, most were insignificant peripherals (97.67%), 44 were module hubs and 34 were connectors (Table S2). No network hub was detected. When correlating node significance to OTU relative abundances (Figure S2B), we found that abundance did not necessarily determine its network significance, although keystone nodes turned to be sparse OTUs. Of the 78 keystone nodes, 31 were rare ( $< 0.1\%$  relative abundance), 27 were moderately rare (0.1-0.5%), 13 were moderately abundant (0.5-1%), and only 7 were considered abundant ( $>1\%$ ). In addition, the relative abundances of module hubs and connectors indicated no significant difference ( $P > 0.05$ ).

**Table S2. Statistics of network keystone nodes.**

Subgroup	Nodes	Peripherals	Module hubs	Connectors	Network hubs	Keystone nodes
0-C	436	427	6	3	0	9 (2.06%)
4-C	472	463	6	3	0	9 (1.91%)
8-C	416	401	6	9	0	15 (3.61%)
16-C	414	403	5	6	0	11 (2.66%)
32-C	406	397	5	4	0	9 (2.22%)
0-N	308	300	3	5	0	8 (2.60%)
4-N	336	330	6	0	0	6 (1.79%)
8-N	280	273	4	3	0	7 (2.50%)
16-N	190	188	1	1	0	2 (1.05%)
32-N	94	92	2	0	0	2 (2.13%)

**Correlation of keystone taxa and their relative abundances.** Most keystone nodes could be assigned to a phylum (85.5%) but only 28.9% could be assigned to a genus. Members of phylum *Proteobacteria* (e.g. genus *Smithella* and *Syntrophorhabdus*) and *Chloroflexi* (genus *Bellilinea*, *Leptolinea* and *Pelolinea*) constituted the majority of keystone taxa. In addition, four keystone nodes were methanogens (Lee et al., 2015), all of which were archaea, members of phylum Euryarchaeota, genus *Methanolinea*, *Methanotherix*, and *Methanobacterium*. We did not identify a correlation of taxonomy to the keystone types; a genus could be a module hub of a network and meanwhile a connector of another

network. For example, genus *Smithella* appeared 5 times in Figure S3, as a module hub in networks of 8-C, 32-C, 4-N, 16N, and also a connector of 8-C.

Phylum *Proteobacteria* and *Chloroflexi* constituted two thirds of the keystone taxa (Figure S4). The rest either belonged to minor phyla (<10% relative abundance) or could not be assigned to any phylum. However, it was inconclusive that members of the two phyla were more likely to be keystone nodes, because the two phyla were meanwhile the dominant phyla in abundance (Figure 2D), and this coincidence masked possible taxonomic preference. Investigation on keystone taxa at the genus level (Figure S3) failed to identify any taxonomic preference, either.

Previously we reported the dominance of genus *Thiobacillus* in the late nitrate communities, but it was never a keystone genus. In the 32-N community where it accounted for 60.88% relative abundance, it had merely 2 negative covariations with two nodes (unclassified *Marinilabiliaceae* and *Bacteroidales*) in the corresponding 32-N network. In fact, it was not sustaining substantial positive or negative covariations with any taxa in any network (Table S3), regardless of abundance. Similarly, *Luteimonas* accounted for 11.36% relative abundance in the 32-N network but was never a keystone genus.

**Table S3. The insignificant connectivity of Genus *Thiobacillus* in all networks.**

Network	(+) links	(-) links	Target
0-C	4	2	Unclassified bacteria and <i>Bacteroidetes</i>
4-C	1	1	Unclassified bacteria
8-C	0	2	Unclassified bacteria
16-C	1	2	Unclassified <i>Firmicutes</i> and <i>Alphaproteobacteria</i> , <i>Candidatus Kuenenia</i>
32-C	2	1	Unclassified bacteria, <i>Turicibacter</i> ,
0-N	1	0	Unclassified <i>Verrucomicrobia</i>
4-N	1	0	<i>Methanosphaerula</i>
8-N	2	1	Unclassified bacteria, <i>Anaerolineaceae</i> , and <i>Deltaproteobacteria</i>
16-N	0	1	<i>Sulfobacillus</i>
32-N	0	2	Unclassified <i>Marinilabiliaceae</i> and <i>Bacteroidales</i>

**The cryptic electron donor.** Elevated nitrate stimulated sulfide and Fe(II) oxidation, but more nitrate in stoichiometry (~40%) was consumed than the sum consumption of AVS and Fe(II) if N<sub>2</sub> was the end product (denitrification). We once hypothesized TOC to be the cryptic electron donor because microbial denitrification driven by oxidation of organic carbon (e.g. glucose, glycerol, formate and some aromatic compounds) is extensively reported (Hunter, Mills, & Kostka, 2006; Reyes-Avila, Razo-Flores, & Gomez, 2004; Seo & DeLaune, 2010; Viridis, Rabaey, Rozendal, Yuan, & Keller, 2010). Furthermore, our previous pilot-scale project (an *in situ* bioremediation of a contaminated creek by nitrate injection) also detected enriched abundances of genes involved in TOC degradation (Xu et al., 2014). The late community compositions however, rejected this hypothesis because the community majority (~70%, sum relative abundance of *Thiobacillus* and *Luteimonas*) were obligate chemoautotrophs, incapable of utilizing organic carbon as energy or carbon sources. Perhaps TOC utilizers were once stimulated by elevated nitrate but were eventually outcompeted in the competition with denitrifiers.

**Auxotroph and Cross-feeding shaped complex communities.** How microbial communities assemble,

maintain and react to perturbations partially depends on nutrient requirements for individual members. Those in soil, sediments or human gut have been proved to rely heavily on cross-feeding, e.g. exchange of vitamins, amino acids and electron donors (B. E. L. Morris, Henneberger, Huber, & Moissl-Eichinger, 2013). Joshua et al. observed a taxonomic convergence at family level and a functional convergence at carbon metabolisms when microbial communities from different habitats were incubated under the same condition, where all microorganisms were competing for glucose (Goldford et al., 2018). Such competition did not lead to a dominance of best competitors but instead was stabilized by cross-feeding of non-specific metabolites, and thus created more niches for those less competitive. Species heavily relying on cross-feeding are usually auxotrophs, which are non-dependent units in nutrition and require additional nutrients than corresponding prototrophs (Zengler & Zaramela, 2018).

Auxotrophy may result from the adaptive gene loss from genomes of original prototrophs so that they do not have to synthesize costly metabolites but can obtain them from other prototrophs, auxotrophs or the host (Zomorodi & Segre, 2017). According to the Black Queen Hypothesis (J. J. Morris, Lenski, & Zinser, 2012), this adaptive function loss brings evolutionary benefits. For example, auxotrophs gain access to metabolites they cannot synthesize because of the interspecies exchanges so that communities with auxotrophs being the majority usually have more compact metagenomes than communities with prototrophs being the majority. The energy being saved from synthesis of costly metabolites can converge at core metabolisms and reproduction, leading to enhanced Darwinian fitness (Hays, Patrick, Ziesack, Oxman, & Silver, 2015). What's more, the massive cross-feeding stabilizes a community. Compared with non-cooperating competitors, synthetic communities dominated by cross-feeding species exhibited much enhanced robustness under frequent perturbations (Pande et al., 2014).

In the manuscript we mentioned that the network connectivity was believed highly associated with microbial cross-feeding or metabolic interdependencies. The first support was the positive covariation between network simplification and the decreasing ratio of auxotrophs. In fact, most genera were outcompeted by *Thiobacillus* and *Luteimonas*, both were prototrophs; Then we identified a taxonomic coincidence between published auxotrophs which were proved performing extensive cross-feeding (Embree, Liu, Al-Bassam, & Zengler, 2015; Hubalek et al., 2017; Mee, Collins, Church, & Wang, 2014; Ponomarova & Patil, 2015) and the identified keystone taxa here (Figure S3). Furthermore the predicted abundances of genes concerning microbial cross-feeding (Figure 4) elevated when the community majority shifted from auxotrophs to prototrophs.

**The taxonomic coincidence between published auxotrophs and identified keystone taxa.** It is certain that network simplification results from the loss of keystone node/taxa, but what determines node connectivity remained unclear. We have excluded OTU abundance, which had little correlation with interactive significance. Zengler et al. provided new insight that auxotrophs greatly enhanced community interspecies dependencies by establishing extensive exchanges of electron, carbon, amino acids and vitamins (Hubalek et al., 2017; Zengler & Zaramela, 2018). By cross-matching we identified a taxonomic coincidence between published auxotrophs discovered from anaerobic environments and the keystone taxa discovered in this study. Some were syntrophic bacteria (e.g. genus *Smithella*, and *Syntrophorhabdus*) and some were methanogenic archaea (e.g. genus *Methanolinea*) (Embree et al., 2015; Hubalek et al., 2017; Mee et al., 2014; Ponomarova & Patil, 2015). Not all keystone nodes

happened to be auxotrophs since a lot of them were unclassified (Figure S3), but auxotrophs were very likely to be keystone nodes.

**Suppression of auxotrophs led to simplified microbial interactions.** Recall that control communities were dominated by methanogens and syntrophic bacteria, both were sensitive to reactants of high redox potential. Nitrate injection had overwritten the sediment chemical characteristics. Consequently, nitrate reducers and AVS oxidizers (e.g. *Thiobacillus* and *Luteimonas*) gained metabolic fitness, and their enrichment decreased the community biodiversity by outcompeting methanogens and syntrophic bacteria, a lot of which were the native auxotrophs (Figure 5A,5B). *Thiobacillus* and *Luteimonas* were both prototrophs and no cross-feeding behavior had yet been reported (Fan, Yu, Li, & Zhang, 2014; Kelly & Wood, 2000).

**Elevated cross-feeding genes supported suppression of auxotrophs.** The predictive general metabolism (Figure 6) indicated that late nitrate communities (16-N and 32-N) differed most from control and early nitrate communities in the elevated abundances of genes concerning metabolisms of rare amino acids, vitamins, cofactors and nucleotides. These were all common metabolites being extensively exchanged in cross-feeding. This is because the community majority had shifted from auxotrophs to prototrophs. As a result, prototrophic members carrying a complete set of metabolic genes for themselves elevated the gene abundances.

### Sequence denoising versus OTU clustering

When this manuscript is about to complete, there have been improved analytical tools. For example, *QIIME2* platform (Bolyen et al., 2019) employs denoising pipelines by *DADA2* (Callahan et al., 2016) and *Deblur* (Amir et al., 2017), which generates amplicon sequence variants (ASVs) rather than classic OTUs. Meanwhile, Robert Edgar supplemented *Unoise* (also a denoising algorithm) to *Usearch*, which generates zero-radius OTUs (zOTUs, similar to ASVs). Denoising pipelines bring single-nucleotide resolution to sequences (Thompson et al., 2017) and well exclude spurious sequences from biological sequences.

We wondered how the denoised sediment microbial community compositions would be different, so we compared the communities constructed by the OTU clustering or *DADA2*. Two methods yielded almost identical community compositions at the phylum-level (Figure S7). At the class-level however, there were several differences, and the most significant one was the disappearance of Class Beta-proteobacteria, where *Thiobacillus* used to belong. This was because of the frequent adjustments of the Silva database. Previously in OTU clustering, we used RDP classifier for taxonomic assignment. In *DADA2* however, RDP classifier is unavailable and Silva is the default taxonomy database.

The version of Silva database employed on our server is release 132. Taking *Thiobacillus* as an example, its taxonomic classification in Silva database changed several times (Table S4). Luckily, these changes did not reach the family or genus level. Therefore, the community compositions constructed by *DADA2* still supported previously conclusions related to community structures, for example:

- The majority of microorganisms (~2/3) could not be assigned to a specific genus;
- Original communities were dominated by methanogens and syntrophic sulfate reducers;
- *Thiobacillus* and *Luteimonas* were significantly enriched by elevated nitrate;

- Original dominant genera were inhibited after nitrate amendment.

**Table S4. Changes of the taxonomic classification of *Thiobacillus* among RDP and Silva databases.**

Level	RDP release 2.11 (updated on 2016-7-12)	Silva release 132 (updated on 2017-12-13)	Silva release 138 (updated on 2019-12-16)
Domain	<i>Bacteria</i>	<i>Bacteria</i>	<i>Bacteria</i>
Phylum	<i>Proteobacteria</i>	<i>Proteobacteria</i>	<i>Proteobacteria</i>
Class	<i>Beta-proteobacteria</i>	<i>Gamma-proteobacteria</i>	<i>Gamma-proteobacteria</i>
Order	<i>Hydrogenophilales</i>	<i>Betaproteobacteriales</i>	<i>Burkholderiales</i>
Family	<i>Hydrogenophilaceae</i>	<i>Hydrogenophilaceae</i>	<i>Hydrogenophilaceae</i>
Genus	<i>Thiobacillus</i>	<i>Thiobacillus</i>	<i>Thiobacillus</i>

## References

- Allen, H. E., Fu, G. M., & Deng, B. L. (1993). Analysis of Acid-Volatile Sulfide (AVS) and Simultaneously Extracted Metals (SEM) for the Estimation of Potential Toxicity in Aquatic Sediments. *Environmental Toxicology and Chemistry*, 12(8), 1441-1453. doi:10.1897/1552-8618(1993)12[1441:Aoasaa]2.0.Co;2
- Amir, A., McDonald, D., Navas-Molina, J. A., Kopylova, E., Morton, J. T., Xu, Z. Z., . . . Knight, R. (2017). Deblur Rapidly Resolves Single-Nucleotide Community Sequence Patterns. *Msystems*, 2(2). doi:10.1128/mSystems.00191-16
- Bolyen, E., Rideout, J. R., Dillon, M. R., Bokulich, N. A., Abnet, C. C., Al-Ghalith, G. A., . . . Asnicar, F. (2019). Reproducible, interactive, scalable and extensible microbiome data science using QIIME 2. *Nature biotechnology*, 37(8), 852-857.
- Callahan, B. J., McMurdie, P. J., Rosen, M. J., Han, A. W., Johnson, A. J. A., & Holmes, S. P. (2016). DADA2: high-resolution sample inference from Illumina amplicon data. *Nature methods*, 13(7), 581.
- Edgar, R. C. (2013). UPARSE: highly accurate OTU sequences from microbial amplicon reads. *Nature methods*, 10(10), 996.
- Embree, M., Liu, J. K., Al-Bassam, M. M., & Zengler, K. (2015). Networks of energetic and metabolic interactions define dynamics in microbial communities. *Proceedings of the National Academy of Sciences of the United States of America*, 112(50), 15450-15455. doi:10.1073/pnas.1506034112
- Fan, X., Yu, T., Li, Z., & Zhang, X.-H. (2014). *Luteimonas abyssi* sp nova, isolated from deep-sea sediment. *International Journal of Systematic and Evolutionary Microbiology*, 64, 668-674. doi:10.1099/ijs.0.056010-0
- Fruchterman, T. M. J., & Reingold, E. M. (1991). Graph Drawing by Force-Directed Placement. *Software-Practice & Experience*, 21(11), 1129-1164. doi:10.1002/spe.4380211102
- Gibbons, S. M., Duvall, C., & Alm, E. J. (2018). Correcting for batch effects in case-control microbiome studies. *Plos Computational Biology*, 14(4). doi:10.1371/journal.pcbi.1006102
- Goldford, J. E., Lu, N., Bajić, D., Estrela, S., Tikhonov, M., Sanchez-Gorostiaga, A., . . . Sanchez, A. (2018). Emergent simplicity in microbial community assembly. *Science*, 361(6401), 469-474.
- Guimera, R., & Amaral, L. A. N. (2005). Cartography of complex networks: modules and universal roles. *Journal of Statistical Mechanics: Theory and Experiment*, 2005(02), P02001.
- Guimera, R., Sales-Pardo, M., & Amaral, L. A. N. (2007). Classes of complex networks defined by role-to-role connectivity profiles. *Nature physics*, 3(1), 63.
- Hays, S. G., Patrick, W. G., Ziesack, M., Oxman, N., & Silver, P. A. (2015). Better together: engineering and

- application of microbial symbioses. *Current Opinion in Biotechnology*, 36, 40-49.
- Hu, Y., & Shi, L. (2014). A Coloring Algorithm for Disambiguating Graph and Map Drawings. In C. Duncan & A. Symvonis (Eds.), *Graph Drawing* (Vol. 8871, pp. 89-100).
- Hubalek, V., Buck, M., Tan, B., Foght, J., Wendeberg, A., Berry, D., . . . Eiler, A. (2017). Vitamin and Amino Acid Auxotrophy in Anaerobic Consortia Operating under Methanogenic Conditions. *Msystems*, 2(5). doi:10.1128/mSystems.00038-17
- Hunter, E. M., Mills, H. J., & Kostka, J. E. (2006). Microbial community diversity associated with carbon and nitrogen cycling in permeable shelf sediments. *Appl. Environ. Microbiol.*, 72(9), 5689-5701.
- Kelly, D. P., & Wood, A. P. (2000). Confirmation of *Thiobacillus denitrificans* as a species of the genus *Thiobacillus*, in the beta-subclass of the Proteobacteria, with strain NCIMB 9548 as the type strain. *International Journal of Systematic and Evolutionary Microbiology*, 50, 547-550. doi:10.1099/00207713-50-2-547
- Lee, S.-H., Park, J.-H., Kim, S.-H., Yu, B. J., Yoon, J.-J., & Park, H.-D. (2015). Evidence of syntrophic acetate oxidation by Spirochaetes during anaerobic methane production. *Bioresource technology*, 190, 543-549.
- Mee, M. T., Collins, J. J., Church, G. M., & Wang, H. H. (2014). Syntrophic exchange in synthetic microbial communities. *Proceedings of the National Academy of Sciences of the United States of America*, 111(20), E2149-E2156. doi:10.1073/pnas.1405641111
- Morris, B. E. L., Henneberger, R., Huber, H., & Moissl-Eichinger, C. (2013). Microbial syntrophy: interaction for the common good. *FEMS microbiology reviews*, 37(3), 384-406.
- Morris, J. J., Lenski, R. E., & Zinser, E. R. (2012). The Black Queen Hypothesis: Evolution of Dependencies through Adaptive Gene Loss. *Mbio*, 3(2). doi:10.1128/mBio.00036-12
- Pande, S., Merker, H., Bohl, K., Reichelt, M., Schuster, S., de Figueiredo, L. F., . . . Kost, C. (2014). Fitness and stability of obligate cross-feeding interactions that emerge upon gene loss in bacteria. *ISME Journal*, 8(5), 953-962. doi:10.1038/ismej.2013.211
- Ponomarova, O., & Patil, K. R. (2015). Metabolic interactions in microbial communities: untangling the Gordian knot. *Current opinion in microbiology*, 27, 37-44.
- Reyes-Avila, J., Razo-Flores, E. a., & Gomez, J. (2004). Simultaneous biological removal of nitrogen, carbon and sulfur by denitrification. *Water Research*, 38(14-15), 3313-3321.
- Seo, D. C., & DeLaune, R. D. (2010). Fungal and bacterial mediated denitrification in wetlands: influence of sediment redox condition. *Water Research*, 44(8), 2441-2450.
- Thompson, L. R., Sanders, J. G., McDonald, D., Amir, A., Ladau, J., Locey, K. J., . . . Earth Microbiome Project, C. (2017). A communal catalogue reveals Earth's multiscale microbial diversity. *Nature*, 551(7681), 457-+. doi:10.1038/nature24621
- Virdis, B., Rabaey, K., Rozendal, R. A., Yuan, Z., & Keller, J. (2010). Simultaneous nitrification, denitrification and carbon removal in microbial fuel cells. *Water Research*, 44(9), 2970-2980.
- Wang, Q., Garrity, G. M., Tiedje, J. M., & Cole, J. R. (2007). Naive Bayesian classifier for rapid assignment of rRNA sequences into the new bacterial taxonomy. *Applied and Environmental Microbiology*, 73(16), 5261-5267. doi:10.1128/aem.00062-07
- Xu, M., Zhang, Q., Xia, C., Zhong, Y., Sun, G., Guo, J., . . . He, Z. (2014). Elevated nitrate enriches microbial functional genes for potential bioremediation of complexly contaminated sediments. *The ISME journal*, 8(9), 1932.
- Zengler, K., & Zaramela, L. S. (2018). The social network of microorganisms - how auxotrophies shape complex communities. *Nature Reviews Microbiology*, 16(6), 383-390. doi:10.1038/s41579-018-0004-5
- Zomorodi, A. R., & Segre, D. (2017). Genome-driven evolutionary game theory helps understand the rise of metabolic interdependencies in microbial communities. *Nature Communications*, 8. doi:10.1038/s41467-017-01407-5